NeuroImage: Clinical 32 (2021) 102846

Contents lists available at ScienceDirect

NeuroImage: Clinical

journal homepage: www.elsevier.com/locate/ynicl

Connectivity correlates to predict essential tremor deep brain stimulation outcome: Evidence for a common treatment pathway

Erik H. Middlebrooks [a,b,*], Lela Okromelidze [a], Joshua K. Wong [c], Robert S. Eisinger [c], Mathew R. Burns [c], Ayushi Jain [a], Hsin-Pin Lin [c], Jun Yu [c], Enrico Opri [d], Andreas Horn [e,i,j], Lukas L. Goede [e], Kelly D. Foote [f], Michael S. Okun [c], Alfredo Quiñones-Hinojosa [b], Ryan J. Uitti [g], Sanjeet S. Grewal [b], Takashi Tsuboi [c,g,h]

[a] Department of Radiology, Mayo Clinic, Jacksonville, FL, USA
[b] Department of Neurosurgery, Mayo Clinic, Jacksonville, FL, USA
[c] Department of Neurology, Norman Fixel Institute for Neurological Diseases, University of Florida, Gainesville, FL, USA
[d] Department of Neurology, Emory University, Atlanta, GA, USA
[e] Movement Disorder and Neuromodulation Unit, Department of Neurology with Experimental Neurology, Charité – Universitätsmedizin Berlin, Corporate Member of Freie Universität Berlin and Humboldt-Universität zu Berlin, Berlin, Germany
[f] Department of Neurosurgery, Norman Fixel Institute for Neurological Diseases, University of Florida, Gainesville, FL, USA
[g] Department of Neurology, Mayo Clinic, Jacksonville, FL, USA
[h] Department of Neurology, Nagoya University Graduate School of Medicine, Nagoya, Japan
[i] Center for Brain Circuit Therapeutics, Department of Neurology, Brigham & Women's Hospital, Harvard Medical School, Boston, MA, USA
[j] Department of Neurosurgery, Massachusetts General Hospital, Harvard Medical School, Boston, MA, USA

ARTICLE INFO

Keywords:
Essential tremor
Deep brain stimulation
Thalamus
Cerebellum

ABSTRACT

Background and purpose: Deep brain stimulation (DBS) is the most common surgical treatment for essential tremor (ET), yet there is variation in outcome and stimulation targets. This study seeks to consolidate proposed stimulation "sweet spots," as well as assess the value of structural connectivity in predicting treatment outcomes.
Materials and methods: Ninety-seven ET individuals with unilateral thalamic DBS were retrospectively included. Using normative brain connectomes, structural connectivity measures were correlated with the percentage improvement in contralateral tremor, based on the Fahn-Tolosa-Marin tremor rating scale (TRS), after parameter optimization (range 3.1–12.9 months) using a leave-one-out cross-validation in 83 individuals. The predictive feature map was used for cross-validation in a separate cohort of 14 ET individuals treated at another center. Lastly, estimated volumes of tissue activated (VTA) were used to assess a treatment "sweet spot," which was compared to seven previously reported stimulation sweet spots and their relationship to the tract identified by the predictive feature map.
Results: In the training cohort, structural connectivity between the VTA and dentato-rubro-thalamic tract (DRTT) correlated with contralateral tremor improvement ($R = 0.41$; $p < 0.0001$). The same connectivity profile predicted outcomes in a separate validation cohort ($R = 0.59$; $p = 0.028$). The predictive feature map represented the anatomical course of the DRTT, and all seven analyzed sweet spots overlapped the predictive tract (DRTT).
Conclusions: Our results strongly support the possibility that structural connectivity is a predictor of contralateral tremor improvement in ET DBS. The results suggest the future potential for a patient-specific functionally based surgical target. Finally, the results showed convergence in "sweet spots" suggesting the importance of the DRTT to the outcome.

Abbreviations: COG, center-of-gravity; DBS, deep brain stimulation; DRTT, dentato-rubro-thalamic tract; dDRTT, decussating portion of the DRTT; ET, essential tremor; FEM, finite element method; FWE, family-wise error; MPRAGE, magnetization-prepared rapid gradient-echo; ndDRTT, non-decussating portion of the DRTT; PSA, posterior subthalamic area; TRS, Fahn-Tolosa-Marin tremor rating scale; VIM, ventral intermediate nucleus; VOp, ventralis oralis posterior nucleus; VTA, volume of tissue activated.

* Corresponding author at: Departments of Radiology and Neurosurgery, Mayo Clinic, 4500 San Pablo Rd, Jacksonville, FL 32224, USA.
E-mail address: middlebrooks.erik@mayo.edu (E.H. Middlebrooks).

https://doi.org/10.1016/j.nicl.2021.102846
Received 6 June 2021; Received in revised form 14 August 2021; Accepted 27 September 2021
Available online 4 October 2021
2213-1582/© 2021 The Author(s). Published by Elsevier Inc. This is an open access article under the CC BY-NC-ND license (http://creativecommons.org/licenses/by-nc-nd/4.0/).

1. Introduction

Essential tremor (ET) is one of the most common movement disorders worldwide, with an estimated prevalence of 0.9% (Louis and Ferreira, 2010). Almost half of individuals with ET will fail pharmacological therapy and require alternative treatments (Thanvi et al., 2006; Louis et al., 2010). Deep brain stimulation (DBS) is well-established as the most common surgical treatment for ET. Despite widespread use, there continues to be variation in targeting approaches, as well as a failure to converge on a single therapeutic target or pathway (Okun et al., 2005).

Thalamic DBS for ET has traditionally targeted the ventral intermediate nucleus (VIM) region of the thalamus. More recently, there has been increasing interest in the posterior subthalamic area (PSA), including the caudal zona incerta, but superiority of one target over others has yet to be unequivocally proven (Eisinger et al., 2018; Fytagoridis et al., 2012; Holslag et al., 2018; Sandvik et al., 2012). Moreover, recent studies have also postulated the existence of stimulation "sweet spots" more anteriorly in the region of the ventralis oralis posterior nucleus (VOp) or along the VIM/VOp border (Middlebrooks et al., 2018; Middlebrooks et al., 2018; Elias et al., 2021; Kim et al., 2018; Pouratian et al., 2011; Tsuboi et al., 2021). The heterogeneity between these targeting sweet spots has left gaps in our understanding of a potential ideal treatment target.

Brain connectivity, as assessed by MRI, has been increasingly explored to understand and to predict DBS outcomes in ET. These studies have collectively observed that stimulation in the cerebello-thalamo-cortical motor network may be responsible for improved tremor control (Middlebrooks et al., 2018; Middlebrooks et al., 2018; Tsuboi et al., 2021; Coenen et al., 2011; Coenen et al., 2020; Coenen et al., 2017; Coenen et al., 2011; Al-Fatly et al., 2019; Akram et al., 2018; Fenoy and Schiess, 2017; Fenoy and Schiess, 2018; Anthofer et al., 2017). A critical component of this network has been historically referred to as the dentato-rubro-thalamic tract (DRTT). The traditional description of this tract is one that connects the dentate nucleus with the contralateral thalamus and motor cortex; however, these fibers do not synapse within the red nucleus despite their name (Middlebrooks et al., 2020). While these decussating fibers (dDRTT) constitute the majority of the DRTT, the existence of a smaller non-decussating portion (ndDRTT) has been recently shown by MRI diffusion tractography and human histological studies (Tsuboi et al., 2021; Middlebrooks et al., 2020; Meola et al., 2016; Petersen et al., 2018; Tacyildiz et al., 2021). These decussating and non-decussating fibers have been shown to possess a distinct spatial gradient within the thalamus, with the dDRTT fibers in general situated more anteriorly (Tsuboi et al., 2021; Middlebrooks et al., 2020; Petersen et al., 2018).

Converging evidence highlights the potential of connectivity-based targeting and programming for ET DBS. However, previous studies have been limited by small sample size or the use of bilateral electrodes. The inclusion of bilateral DBS electrodes has the potential to confound the observed tremor improvement due to the potential for unpredictable ipsilateral effects or unequal tract activation between the hemispheres (Noecker et al., 2021). We aimed to show that structural connectivity could be predictive of ET DBS outcome through modulation of the cerebello-thalamo-cortical motor network in a large cohort of unilateral ET DBS individuals. The predictive connectivity fingerprints from this cohort were then used for validation in a second cohort drawn from another institution. Additionally, we assessed the stimulation "sweet spot" and compared it to existing reported "sweet spots." We sought to either confirm or deny the potential existence of a common tract unifying the "sweet spots" reported in the literature.

2. Methods

2.1. Study design

This multicenter, retrospective cohort study was approved by the Institutional Review Boards of the University of Florida and Mayo Clinic Florida. The inclusion criteria of the present study were (1) diagnosis of essential tremor defined by the Movement Disorders Society (isolated tremor syndrome of bilateral upper limb action tremor with or without tremor in other body regions) (Bhatia et al., 2018); (2) unilateral thalamic DBS implantation, (3) preoperative clinical evaluation using the Fahn-Tolosa-Marin tremor rating scale (TRS), (4) postoperative TRS after DBS programming optimization, (5) preoperative brain MRI including a high-resolution, T1-weighted magnetization-prepared rapid gradient-echo (MPRAGE) sequence and high-resolution postoperative CT, (6) absence of other brain surgeries, and (7) absence of secondary etiologies for tremor or neurodegenerative diseases. We excluded individuals with tremor syndromes with additional features of parkinsonism, ataxia, myoclonus, or questionable dystonia (i.e., essential tremor plus). We identified 83 ET individuals in the training cohort from the University of Florida and 14 in the validation cohort from Mayo Clinic Florida meeting the inclusion criteria (total of 97 individuals included).

2.2. Perioperative procedures and assessments

As the standard of care at the University of Florida and Mayo Clinic Florida, all the patients underwent unilateral DBS implantation, and staged implantation of the other side was considered later. In this study, tremor outcomes were assessed using the scores when the patients were treated only with unilateral DBS. Imaging protocols have been previously described (Middlebrooks et al., 2018), and are also summarized in Supplemental Methods. Perioperative procedures and assessments for ET individuals from the University of Florida cohort have also been previously described (Tsuboi et al., 2021). Briefly, DBS leads were implanted in the University of Florida cohort under local anesthesia with intraoperative microelectrode recordings and macrostimulation testing. Using in-house software (Morishita et al., 2010), we aimed to place the electrode at the VIM/VOp border with the most ventral contact deep to the thalamus and the dorsal contacts in the posterior aspect of the VOp.

Individuals recruited from the Mayo Clinic cohort were selected from the Mayo Clinic Movement Disorders Neurology Clinic after decision to undergo unilateral VIM DBS for ET. After application of a stereotactic headframe, a stereotactic CT was performed. The CT images were co-registered to the preoperative MRI on the surgical planning workstation. Using Guiot's relationships to target the Vim, an initial target was planned at the level of the anterior commissure-posterior commissure (AC-PC) and one-fourth the AC–PC distance anterior to the PC. A lateral coordinate equal to the sum of one-half the width of the third ventricle plus 11.5 mm was initially selected. The electrode was advanced through a burr hole with the patient in a semisitting position with 30-degree head elevation. Macrostimulation was performed to assess tremor improvement and thresholds for stimulation of the internal capsule, paresthesias, speech disturbances, or other adverse effects. If tremor control was adequate without adverse effects, no further adjustments were made. If the result was unsatisfactory, the electrode was repositioned according to the stimulation effect obtained. Implants included the model 3387 lead and pulse generator (Activa PC/SC or Soletra; Medtronic Inc, Minneapolis, MN, USA) or an 8-contact lead or directional lead and pulse generator (Vercise or Vercise Cartesia; Boston Scientific Corp, Marlborough, MA, USA). Approximately 3 months after surgery, high-resolution CT was obtained using a dual-energy protocol (80 kV and 150 kV) with an in-plane resolution of 0.5×0.5 mm and slice thickness of 0.4 mm.

For both cohorts, monthly visits were scheduled to optimize stimulation parameters. Optimization was typically achieved within 6 months of initial programming. An itemized TRS score was assessed by a skilled examiner prior to surgery and after programming optimization using the optimized programming settings. The contralateral tremor score was calculated from the lateralized TRS motor scores (items 5, 6, 8, 9, and 11–14) on the body side contralateral to the DBS. Percentage

improvement in contralateral tremor score from preoperative baseline to optimized postoperative assessment was the primary outcome measure.

2.3. Image processing

A forked version of the Lead-DBS software package (http://www.lead-dbs.org) (Horn et al., 2019) was used for electrode localization and estimation of volumes of tissue activated (VTA). Lead-DBS was modified to integrate functionality for unilateral electrodes, and the code used is freely available (https://github.com/oprienrico/leaddbs_dev/tree/dev_patched). Modifications have now been integrated to the main branch and are available from Lead-DBS v2.5 onwards.

The high-resolution postoperative CT images were coregistered to preoperative MPRAGE images using a two-stage linear registration in Advanced Normalization Tools (http://stnava.github.io/ANTs/) (Avants et al., 2008). The images were then normalized into MNI_ICBM_2009b_NLIN_ASYM space—based on the MPRAGE images—with the SyN registration method in Advanced Normalization Tools (Avants et al., 2008; Fonov et al., 2011). A five-stage nonlinear transform was applied: two linear (rigid and affine) registrations, whole-brain nonlinear SyN-registration, and two nonlinear SyN-registrations with a focus on subcortical nuclei (Schönecker et al., 2009). A subsequent affine transform that was restricted to subcortical regions of interest was performed to ensure accurate subcortical registration (Horn et al., 2019). Electrodes were localized using an automated and phantom-validated approach implemented in Precise and Convenient Electrode Reconstruction for Deep Brain Stimulation (PaCER) (Husch et al., 2018) and, after manual adjustment, visually inspected for accuracy.

Using a finite element method (FEM)-based model in Lead-DBS (Horn et al., 2019), a VTA was estimated for each patient's optimized programming settings. The E-field was estimated on a tetrahedral mesh that includes two tissue compartments (gray and white matter), insulating components, and electrode contacts. Conductivity values were adapted for the range of frequencies used in this cohort: 0.092 S/m and 0.06 S/m for gray and white matter conductivity, respectively. A modified FieldTrip-SimBio pipeline, implemented in Lead-DBS, was used to estimate the E-field distribution with VTA shape based on a typical threshold of >0.2 V/mm (Astrom et al., 2015; Vorwerk et al., 2018). The right hemisphere VTAs were nonlinearly flipped to the left hemisphere.

2.4. VTA analysis

Stimulation sweet spot was assessed for percentage improvement in contralateral tremor score using modifications of methods in Dembek et al. (2017). The binary left hemisphere and mirrored right hemisphere VTAs were multiplied by the subject's percentage improvement to create a weighted improvement mask. The weighted improvement mask was then averaged to generate an improvement heat map. Next, a mask for statistical significance was created using the masked weighted VTAs in a voxel-wise, two-sided non-parametric permutation test using 10,000 permutations. Due to the large number of voxels in regions well beyond the area of stimulation, p values from statistical tests can be artifactually improved by the excessive directions of freedom. To account for this, all zero voxels and those voxels with VTA overlap in less than 15% of subjects were excluded from analysis. The significance mask was generated for only those voxels with FWE-corrected $p < 0.05$ and applied to the average improvement heat map. The sweet spot was determined by assessing the cluster center-of-gravity (COG) for the resulting heat map.

2.5. Structural connectivity processing

The left hemisphere and mirrored right-hemisphere VTAs were used as seeds for structural connectivity assessment. A normal control dataset of 124 healthy subjects in the Human Connectome Project (https://www.humanconnectome.org) (Setsompop et al., 2013) was utilized, as detailed in Tsuboi et al. (2021) For each VTA, probabilistic tractography was performed using "probtrackx2_gpu" from the FMRIB Software Library v6.0.3 (http://fsl.fmrib.ox.ac.uk) in each of the 124 subjects with 20,000 samples, curvature threshold of 0.2, modified Euler streamlining, and step length of 0.5 mm. A region-of-avoidance included the hemisphere contralateral to the VTA and corpus callosum. The resultant probability paths were averaged for all 124 control subjects giving an averaged probability map for each subject's VTA.

2.6. Structural connectivity analysis – training dataset

Next, to assess whether the probability distribution was predictive of improvement in the 83-patient training cohort, a leave-one-out cross validation was performed using the averaged probability map for each subject. We treated this probability distribution analogously as connectivity *fingerprints* seeding from DBS stimulation sites. Group R-maps (voxel-wise correlations of fingerprint values with clinical improvement values) were generated with all individuals except one, which was withheld for validation. The structural connectivity fingerprint for the left-out patient was then again used to measure spatial similarity with the R-map generated from the remainder of the cohort (using spatial correlations). Pearson correlation was performed using the similarity index versus measured clinical improvement and $p < 0.05$ was considered statistically significant.

2.7. Structural connectivity analysis – validation dataset

To assess generalizability of the predictions, the structural connectivity fingerprint for each patient in the 14-patient validation dataset was used to measure spatial similarity with the R-map generated from the complete 83-patient training cohort (same process as in the cross-validation step). Pearson correlation was performed using the similarity index versus measured clinical improvement and $p < 0.05$ was considered statistically significant.

2.8. Comparison to previous sweet spots

To assess spatial location of the VTA sweet spot for contralateral tremor improvement in the current cohort, as well as comparison of previously reported targets (Elias et al., 2021; Tsuboi et al., 2021; Al-Fatly et al., 2019; Akram et al., 2018; Papavassiliou et al., 2004; Middlebrooks et al., 2021; Kübler et al., 2021), each of the previously reported MNI sweet spots (Table 2) were plotted in relation to the predictive tract *fingerprint.* The R-map derived from the training cohort was thresholded at $R > 0.1$ and the distance from each coordinate to the nearest predictive voxel was calculated as a 3D Euclidean distance.

2.9. Statistical analysis

Subject demographics, baseline scores, postoperative improvement, and DBS parameters were expressed as mean and SD. Comparison between the training and validation cohorts was performed using a nonparametric Mann-Whitney U test.

2.10. Data availability

Data are available upon specific request pending a formal data sharing agreement and approval from the authors' and requesting researcher's local ethics committees.

3. Results

3.1. Clinical outcomes

Demographic and clinical information are summarized in Table 1. All individuals underwent unilateral thalamic DBS with a mean follow-up period of 6.8 ± 1.5 months (range 3.1–12.9 months). There was no significant difference in the age at surgery, sex, or age of onset between the cohorts ($p > 0.05$); however, the disease duration was greater in the training cohort (28.4 vs. 18.4 years; $p = 0.04$). Total TRS score at baseline was greater in the training cohort compared to the validation cohort (51.3% vs. 42.8%; $p = 0.003$), but contralateral TRS tremor score was not significantly different (16.3% vs. 16.1%; $p = 0.97$). Likewise, there was a similar observed improvement in contralateral TRS score after surgery between the training and validation cohort (71.4% vs. 69.1%; $p = 0.72$).

3.2. VTA analysis

The electrode contact positions relative to VIM and VOp from the DBS Intrinsic Atlas (DISTAL) (Ewert et al., 2018) are shown for the training cohort in Fig. 1A and the validation cohort in Fig. 1B. The active contact positions for the training cohort color-coded by contralateral tremor improvement are shown relative to VIM and VOp (Fig. 1C) and to dDRTT (Fig. 1D). The masked weighted VTA heat maps for contralateral tremor improvement are shown in Fig. 2. The cluster peak COG for contralateral tremor improvement was along the ventral VIM/VOp border (MNI = −15.5/−15.5/0.5) in the training cohort and was more medial and superior in the validation cohort (MNI = −13.5/−15.5/2).

3.3. Structural connectivity analysis

The mean structural connectivity for the training cohort is shown in Fig. 3A and shows greatest connectivity to the primary motor, sensory, supplementary motor, and premotor cortices. A similar pattern of mean connectivity is seen in the validation cohort (Fig. 3B).

In the training cohort, a leave-one-out cross validation shows that connectivity *fingerprint* is predictive of contralateral tremor improvement within the cohort ($r = 0.41$; $p < 0.0001$). The group R-map (Fig. 3D-3F) shows that the voxels most predictive of contralateral tremor improvement correspond to the DRTT. In cross-validation with the separate validation cohort (Fig. 3G), the connectivity fingerprint from the training cohort was predictive of tremor improvement ($r = 0.59$; $p = 0.025$).

Table 1
Baseline patient characteristics and DBS outcomes.

	Training Cohort n = 83	Validation Cohort n = 14	p value
Age at DBS (years)	68.2 ± 9.9	69.1 ± 8.4	0.81
Disease duration before DBS (years)	28.4 ± 17.7	18.4 ± 15.1	0.04
Age at onset (years)	39.8 ± 20.7	50.8 ± 13.6	0.07
Sex (male, %)	65.1%	42.9%	0.14
TRS total score at baseline	51.3 ± 14.8	42.8 ± 10.2	0.003
Contralateral TRS tremor score at baseline*	16.3 ± 4.7	16.1 ± 4.4	0.97
TRS total score improvement after DBS (%)	54.7 ± 21.2	–	
Contralateral TRS tremor score improvement after DBS (%)	71.4 ± 22.2	69.1 ± 24.1	0.72
Follow-up period after DBS (months)	6.8 ± 1.5	7.1 ± 1.9	
Monopolar / Bipolar stimulation	54 / 29	2 / 12	
Stimulation voltage (V)	2.5 ± 0.8	3.1 ± 1.0	0.01
Stimulation pulse width (μs)	97.2 ± 23.4	74.3 ± 13.4	<0.0001
Stimulation frequency (Hz)	149.1 ± 21.2	149.6 ± 21.2	0.29

Data are presented as mean ± SD unless otherwise indicated. DBS = deep brain stimulation; TRS = Fahn-Tolosa-Marin Tremor Rating Scale.
* Contralateral TRS motor scores indicate lateralized scores contralateral to DBS implantations. Items 5, 6, 8, 9, and 11–14.
Total TRS Score not available for validation cohort due to lack of TRS Part C on follow up.

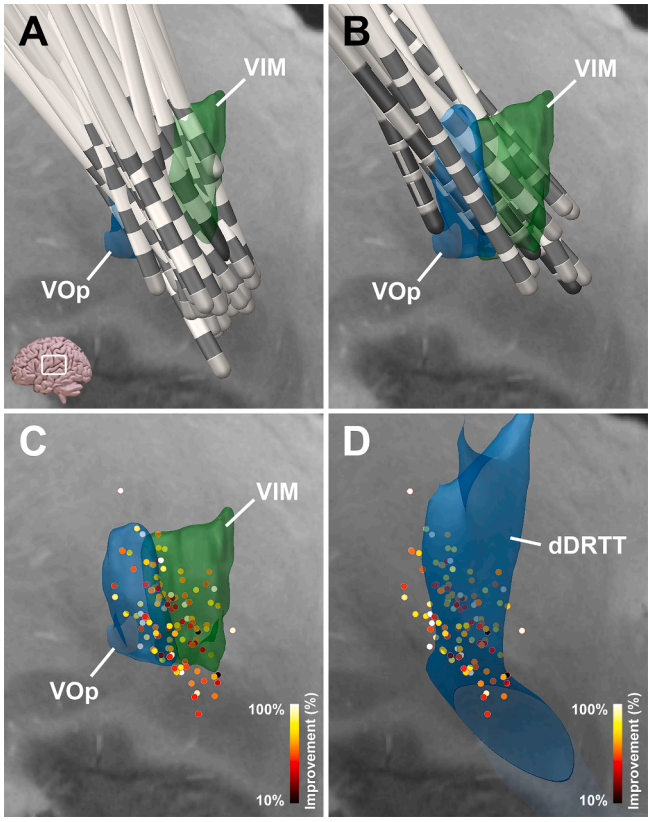

Fig. 1. Sagittal image showing the relationship of electrodes in the training cohort (A) and validation cohort (B) relative to the ventral intermediate nucleus (VIM) and ventralis oralis posterior (VOp) nucleus from the DISTAL atlas (Ewert et al., 2018). (C) Active contacts weighted by percentage improvement in contralateral tremor relative to VIM and VOp. (D) Active contacts weighted by percentage improvement in contralateral tremor relative to the decussating portion of the dentato-rubro-thalamic tract (dDRTT). Background brain template provided by Edlow et al. (2019).

3.4. Comparison to previous sweet spots

Comparison of the current stimulation sweet spot with multiple existing published sweet spots (Table 2) showed a mean distance of 0 ± 0 mm, meaning that every reported coordinate overlapped with the predictive tract derived from the training cohort (Fig. 4A & 4B).

4. Discussion

Our study revealed that a structural connectivity fingerprint was an independent predictor of contralateral tremor improvement within our training cohort, as well as predictive of improvement in a separate independent cohort. Further, we showed that the heterogeneity in recently reported stimulation "sweet spots" can potentially be explained by their distance to a common pathway, the dentato-rubro-thalamic tract.

The strengths of our study included the use of unilateral electrodes, which minimized potential confounds from ipsilateral microlesion effects from a second DBS electrode on the measurement of contralateral tremor change. Unilateral implants also facilitated the evaluation of pure ipsilateral change in tremor without similar confounds. It is possible that a higher incidence of stimulation-induced side effects in

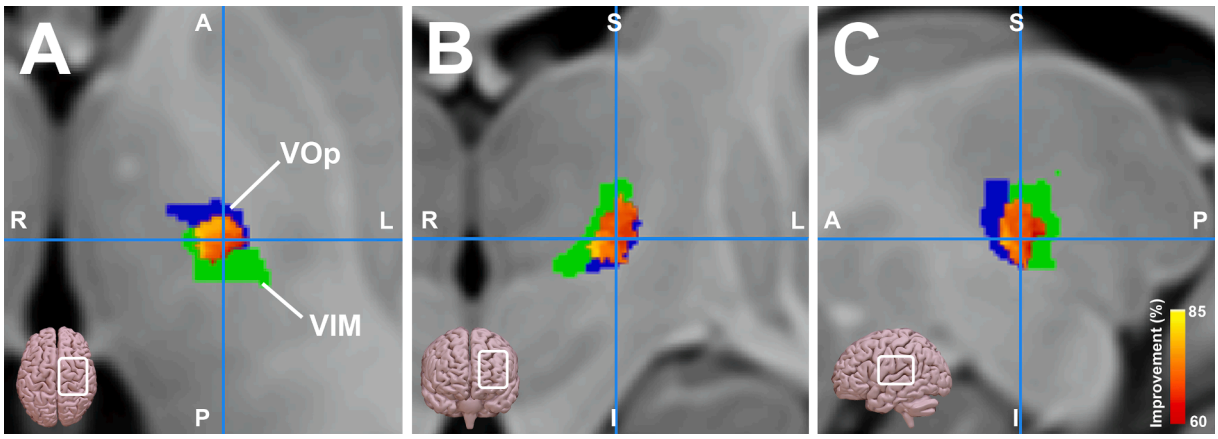

Fig. 2. Statistically significant average improvement heat map for percentage improvement in contralateral tremor score (A, axial; B, coronal; and C, sagittal views) relative to the ventral intermediate nucleus (VIM; green) and ventralis oralis posterior (VOp; blue) from the DISTAL atlas (Ewert et al., 2018). Crosshairs show the cluster center of gravity indicating the point of greatest improvement. (For interpretation of the references to color in this figure legend, the reader is referred to the web version of this article.)

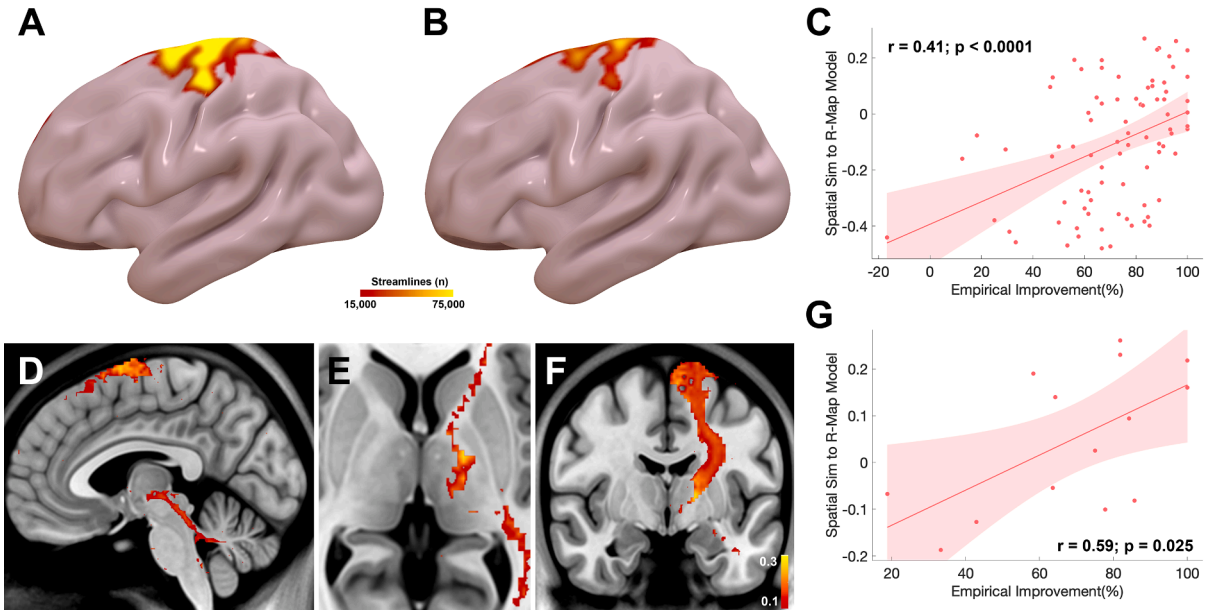

Fig. 3. Results of structural connectivity analysis for the training cohort (A) and validation cohort (B). (C) Scatterplot illustrates the correlation between the empirical improvement in contralateral tremor compared to similarity to the predictive R-map for each subject from the leave-one-out cross-validation ($r = 0.41$; $p < 0.0001$). Sagittal (D), axial (E), and coronal (F) images show the tract most correlated with contralateral tremor improvement with greatest correlation seen with the DRTT. (G) Scatterplot shows cross-validation results for the validation cohort from a second institution based on the connectome fingerprints from the training cohort showing that the training cohort is predictive of outcomes in the second cohort ($r = 0.59$; $p = 0.025$).

bilateral implants could influence the choice of stimulation parameters and this could have introduced bias into our study. Despite this limitation, we report the largest ET cohort, to our knowledge (N = 97), to undergo both connectivity and VTA analysis. Our results add a new dimension to the several prior small studies and bilateral implant cohorts (Middlebrooks et al., 2018; Middlebrooks et al., 2018; Coenen et al., 2011; Coenen et al., 2020; Coenen et al., 2017; Coenen et al., 2014; Coenen et al., 2011; Al-Fatly et al., 2019; Akram et al., 2018; Fenoy and Schiess, 2017; Fenoy and Schiess, 2018; Anthofer et al., 2017).

Our results show that contralateral TRS motor improvement was predicted by structural connectivity to the DRTT. The predictive maps revealed were consistent with those described by Al-Fatly et al. (Al-Fatly et al., 2019) The DRTT has traditionally been described as efferent cerebellar fibers extending from the dentate nucleus through the ipsilateral superior cerebellar peduncle before decussating in the midbrain to reach the contralateral VIM and VOp, and ending in the contralateral primary motor cortex (Petersen et al., 2018; Gallay et al., 2008). Subsequently, a smaller portion of the DRTT consisting of fibers extending from the dentate nucleus to the ipsilateral thalamus and motor cortex without decussating, the ndDRTT, were shown in animal and human histological studies (Tacyildiz et al., 2021; Flood and Jansen, 1966; Wiesendanger and Wiesendanger, 1985). These findings have been supported by more recent exploration using MRI tractography and brain microdissection in human (Middlebrooks et al., 2020; Meola et al., 2016; Petersen et al., 2018; Tacyildiz et al., 2021). These ndDRTT fibers make up a minority of the DRTT (<25% of tracts) (Meola et al., 2016) and their role in tremor has not been well established. Converging evidence from functional and anatomical studies shows a lateral and posteromedial motor region of the dentate nucleus, which contributes a

Table 2
Summary of studies reporting stimulation "sweet spots."

Reference	Study Type	Electrode Side (Unilateral/ Bilateral)	Number of Patients	Mean Follow-up (mos)	MNI Sweet Spot Coordinates (x/ y/z)	Outcome Scores Reported	Baseline Total TRS Score (mean)	Total TRS Percentage Improvement (mean)
Elias et al. (2021)	Retrospective Cohort	Unilateral	39	16.8	−17.3 / −13.9 / 4.2	Total TRS	57.2	42.8%
Tsuboi et al. (2021)	Retrospective Cohort	Unilateral	20	6.6	−15 / −17 / 1	Total TRS*, TRS Motor Score, Contralateral TRS Motor Score	54.2	58.0%
Al-Fatly et al. (2019)	Retrospective Cohort	Bilateral	36	12	−16 / −20 / −2	Total TRS, Head Tremor Score, Contralateral UE Score	33.3	65.1%
Middlebrooks et al. (2021)	Prospective, Randomized Blinded Trial	Unilateral	6	3	−15 / −18.5 / −2.5	Total TRS	34.3	64.5%
Papavassiliou et al. (2004)	Retrospective Cohort	Unilateral and Bilateral	37	26	−14.5 / −17.7 / −2.8	Limited TRS of Contralateral UE	–	–
**Akram et al. (2018)	Retrospective Cohort	Unilateral	5	23.6	−12.5 / −16 / −3.5	Total TRS	81.6	34.0%
***Kübler et al. (2021)	Retrospective Cohort	Bilateral	30	14	−12 / −19.5 / −5.5	TRS Parts A & B, TRS of Contralateral UE	–	–

MNI = Montreal Neurological Institute template space; TRS = Fahn-Tolosa-Marin Tremor Rating Scale; UE = upper extremity.
* Unpublished data.
** Coordinates approximated from image figures.
*** Point of maximum tremor improvement.

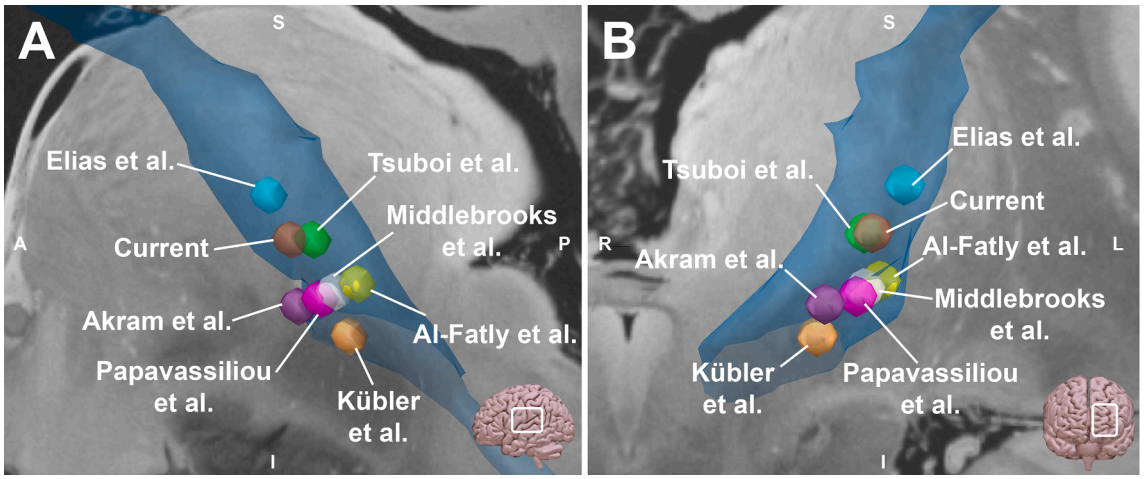

Fig. 4. Relationship of the predictive tract derived from the training cohort (threshold R > 0.1) to the current study sweet spot for contralateral tremor improvement and previously reported tremor sweet spots (Elias et al., 2021; Tsuboi et al., 2021; Al-Fatly et al., 2019; Akram et al., 2018; Papavassiliou et al., 2004; Middlebrooks et al., 2021; Kübler et al., 2021). (A) Sagittal and (B) coronal views show overlap of all targets with the predictive tract, which represents the DRTT. Background provided by Edlow et al. (2019).

majority of fibers to the dDRTT, with a smaller fraction to the ndDRTT, potentially explaining reported ipsilateral motor effects. Meanwhile, the ndDRTT constitutes a large fraction of anteriomedial dentate nucleus fibers, thought to contribute to nonmotor functions (Tacyildiz et al., 2021; Küper et al., 2012; Ellerman et al., 1994; Middleton and Strick, 2000; Middleton and Strick, 1998). Nevertheless, the ndDRTT has been used as a biomarker in several DBS studies, possibly due to challenges in reconstructing crossing fibers of the dDRTT using tractography (Coenen et al., 2016; Sammartino et al., 2016; Coenen et al., 2011; Coenen et al., 2020; Coenen et al., 2017; Coenen et al., 2014; Coenen et al., 2011). This limitation is an important consideration given the variability in the spatial location of these two components. While they are more coherently organized within the ventral thalamic region, the tracts have a more distinct spatial separation in the PSA (Middlebrooks et al., 2020; Petersen et al., 2018). This anatomical distribution provides a critical point for evaluating discrepancies in reporting stimulation "sweet spots" for ET. Unfortunately, distinction between the effects of these tracts from our cohort cannot be completely assessed due to the large amount of overlap of both tracts in the ventral thalamic region, as well as preferential tracking of ndDRTT fibers by tractography algorithms. Future studies will be needed to better understand the role of these two different components of the DRTT.

Recently, connectivity and VTA studies have questioned the traditional mantra of VIM stimulation for tremor control (Middlebrooks et al., 2018; Kim et al., 2018; Pouratian et al., 2011) despite criticism (Akram et al., 2019). Such critiques were based on the traditional concept of nuclear effects rather than the underlying tractographic anatomy. Nevertheless, two of the largest cohorts of ET individuals undergoing VTA sweet spot analysis, the current study and Elias et al. (2021) have both revealed more anterior stimulations along the VIM/VOp border and more anterior stimulations in VOp. These findings are in contradiction to the more posterior location of sweet spots in the more ventral or posterior subthalamic region, which are more closely related to the location of VIM. Our results can potentially reconcile these

variations in reported targeting by revealing a common underlying pathway, the DRTT, along the course of both PSA and ventral thalamic stimulation targets. There was reproducibility of tremor control at various locations along the DRTT (e.g., PSA, VIM/VOp), and may potentially explain observations that more posterior VIM stimulation can lead to tolerance (Sandoe et al., 2018). In addition, our results support the potential of individualized targeting of DRTT, which has been recently shown as feasible and effective in clinical practice (Middlebrooks et al., 2021).

5. Limitations

Several limitations of the present study should be considered. First, clinical assessments were limited to the retrospective analysis of patient records. While metrics used for the study were meticulously documented by experienced examiners, other information regarding side effects or other outcomes may have been less consistent. Along the same lines, the mean and median duration of follow up was slightly more than 6 months, which limits assessment of factors affecting long-term DBS benefit. Second, the use of normative connectomes poses a potential limitation. While there may be pathological alterations in the represented networks in the setting of ET, the diffusion metrics are primarily used in this study from an anatomic perspective only. The anatomic connections from such normative connectomes compared to patient-specific cohorts has been previously shown as a reliable metric (Wang et al., 2021). Prior studies have also supported the use of normative connectomes by their ability to predict both treatment effects and side effects from DBS (Tsuboi et al., 2021; Al-Fatly et al., 2019; Tsuboi et al., 2021; Horn et al., 2017; Baldermann et al., 2019). There were many inherent limitations of tractography that have been previously well described, such as difficulty with modeling crossing fibers and reliability of tracking through regions with lower fractional anisotropy (e.g. thalamic gray matter). We used a more computationally intensive approach of probabilistic tractography, which is more favorable in identifying such plausible tracts, at the risk of increased false fibers. Third, there are inherent limitations from lead localization, co-registration, and normalization processes, as well as the inability to directly visualize most thalamic nuclei on MPRAGE images resulting in a reliance on atlases. Fourth, the presence of connectivity between two regions does not ensure a stimulation effect occurs with specific stimulation parameters (e.g., frequency, pulse width, etc.) (Middlebrooks et al., 2020). Whether all regions connected to a VTA are affected by the chosen stimulation parameters remains speculative. Fifth, the earlier studies analyzed the "sweet spots" for tremor improvement using different methodologies. Therefore, the meta-analysis of the current and earlier studies should be interpreted carefully. Finally, we only included individuals with ET, which limits the extrapolation of our findings to other tremor syndromes.

6. Conclusions

Using a large cohort of individuals with unilateral thalamic DBS, we have shown the potential value of structural connectivity in predicting ET outcomes. Additionally, our results reveal compelling evidence for a common tract, the DRTT as the unifying "sweet spot." We suggest that the provision of a patient-specific network target for direct surgical targeting and device programming has the potential to improve ET DBS outcomes.

CRediT authorship contribution statement

Erik H. Middlebrooks: Conceptualization, Methodology, Software, Formal analysis, Writing - original draft. **Lela Okromelidze:** Conceptualization, Methodology, Software, Data curation, Writing - review & editing. **Joshua K. Wong:** Conceptualization, Methodology, Investigation, Data curation, Writing - review & editing. **Robert S. Eisinger:** Conceptualization, Methodology, Investigation, Data curation, Writing - review & editing. **Mathew R. Burns:** Investigation, Data curation, Writing - review & editing. **Ayushi Jain:** Data curation, Writing - review & editing. **Hsin-Pin Lin:** Investigation, Data curation, Writing - review & editing. **Jun Yu:** Investigation, Data curation, Writing - review & editing. **Enrico Opri:** Conceptualization, Methodology, Software, Formal analysis, Writing - review & editing. **Andreas Horn:** Conceptualization, Methodology, Software, Formal analysis, Writing - review & editing. **Lukas L. Goede:** Conceptualization, Methodology, Software, Formal analysis, Writing - review & editing. **Kelly D. Foote:** Investigation, Writing - review & editing, Supervision. **Michael S. Okun:** Conceptualization, Investigation, Writing - review & editing, Supervision. **Alfredo Quiñones-Hinojosa:** Writing - review & editing, Supervision. **Ryan J. Uitti:** Conceptualization, Writing - review & editing, Supervision. **Sanjeet S. Grewal:** Conceptualization, Methodology, Writing - review & editing, Supervision. **Takashi Tsuboi:** Conceptualization, Methodology, Formal analysis.

Declaration of Competing Interest

Dr. Middlebrooks has received research support from Varian Medical Systems, Inc. and Boston Scientific Corp. He has also received institutional research support from Mayo Clinic and as a Site PI, Co-I, and consultant on NIH supported grants unrelated to the current study. He is also a consultant for Boston Scientific Corp.

Dr. Burns receives salary support from the Parkinson's Foundation.

Dr. Horn was supported by the German Research Foundation (Deutsche Forschungsgemeinschaft, Emmy Noether Stipend 410169619 and 424778381 – TRR 295) as well as Deutsches Zentrum für Luft- und Raumfahrt (DynaSti grant within the EU Joint Programme Neurodegenerative Disease Research, JPND). A.H. is participant in the BIH-Charité Clinician Scientist Program funded by the Charité –Universitätsmedizin Berlin and the Berlin Institute of Health.

Dr. Foote has served as a consultant for Medtronic and Boston Scientific and has received honoraria for these services. He has received research support from Medtronic, Boston Scientific, Abbott/St. Jude, and Functional Neuromodulation. He has received fellowship support from Medtronic.

Dr. Okun serves as a consultant for the National Parkinson Foundation, and has received research grants from NIH, NPF, the Michael J. Fox Foundation, the Parkinson Alliance, Smallwood Foundation, the Bachmann-Strauss Foundation, the Tourette Syndrome Association, and the UF Foundation. Dr. Okun's DBS research is supported by: R01 NR014852 and R01NS096008. Dr. Okun has previously received honoraria, but in the past >60 months has received no support from industry. Dr. Okun has received royalties for publications with Demos, Manson, Amazon, Smashwords, Books4Patients, and Cambridge (movement disorders books). Dr. Okun is an associate editor for New England Journal of Medicine Journal Watch Neurology. Dr. Okun has participated in CME and educational activities on movement disorders (in the last 36) months sponsored by PeerView, Prime, QuantiaMD, WebMD, Medicus, MedNet, Henry Stewart, and by Vanderbilt University. The institution and not Dr. Okun receives grants from Medtronic, Abbvie, Allergan, and ANS/St. Jude, and the PI has no financial interest in these grants. Dr. Okun has participated as a site PI and/or co-I for several NIH, foundation, and industry sponsored trials over the years but has not received honoraria.

Dr. Quiñones-Hinojosa is supported by the Mayo Clinic Professorship and a Clinician Investigator award, and Florida State Department of Health Research Grant, and the Mayo Clinic Graduate School, as well as the NIH (R43CA221490, R01CA200399, R01CA195503, and R01CA216855).

Dr. Grewal is a consultant for Boston Scientific Corp. and Medtronic, Inc.

Acknowledgements

We would like to thank Harith Akram, M.D. for his contribution of prior study data. Mayo Clinic Florida data [in part] were previously collected from study funded by Mayo Clinic Transform the Practice Award. Additional data were provided [in part] by the Human Connectome Project, WU-Minn Consortium (Principal Investigators: David Van Essen and Kamil Ugurbil; 1U54MH091657) funded by the 16 NIH Institutes and Centers that support the NIH Blueprint for Neuroscience Research; and by the McDonnell Center for Systems Neuroscience at Washington University. We acknowledge the Parkinson's Foundation Center of Excellence at the University of Florida and the UF INFORM database.

Funding

This research did not receive any specific grant from funding agencies in the public, commercial, or not-for-profit sectors.

Appendix A. Supplementary data

Supplementary data to this article can be found online at https://doi.org/10.1016/j.nicl.2021.102846.

References

Akram, H., Dayal, V., Mahlknecht, P., Georgiev, D., Hyam, J., Foltynie, T., Limousin, P., De Vita, E., Jahanshahi, M., Ashburner, J., Behrens, T., Hariz, M., Zrinzo, L., 2018. Connectivity derived thalamic segmentation in deep brain stimulation for tremor. Neuroimage Clin. 18, 130–142.

Akram, H., Hariz, M., Zrinzo, L., 2019. Connectivity derived thalamic segmentation: separating myth from reality. Neuroimage Clin. 22, 101758. https://doi.org/10.1016/j.nicl.2019.101758.

Al-Fatly B, Ewert S, Kubler D, et al. Connectivity profile of thalamic deep brain stimulation to effectively treat essential tremor. Brain 2019;142:3086–3098.

Anthofer, J., Steib, K., Lange, M., Rothenfusser, E., Fellner, C., Brawanski, A., Schlaier, J., 2017. Distance between active electrode contacts and dentatorubrothalamic tract in patients with habituation of stimulation effect of deep brain stimulation in essential tremor. J. Neurol. Surg. A Cent. Eur. Neurosurg. 78 (04), 350–357.

Astrom, M., Diczfalusy, E., Martens, H., Wardell, K., 2015. Relationship between neural activation and electric field distribution during deep brain stimulation. IEEE Trans. Biomed. Eng. 62 (2), 664–672.

Avants, B., Epstein, C., Grossman, M., Gee, J., 2008. Symmetric diffeomorphic image registration with cross-correlation: evaluating automated labeling of elderly and neurodegenerative brain. Med. Image Anal. 12 (1), 26–41.

Baldermann, J.C., Melzer, C., Zapf, A., Kohl, S., Timmermann, L., Tittgemeyer, M., Huys, D., Visser-Vandewalle, V., Kühn, A.A., Horn, A., Kuhn, J., 2019. Connectivity profile predictive of effective deep brain stimulation in obsessive-compulsive disorder. Biol. Psychiatry 85 (9), 735–743.

Bhatia, K.P., Bain, P., Bajaj, N., Elble, R.J., Hallett, M., Louis, E.D., Raethjen, J., Stamelou, M., Testa, C.M., Deuschl, G., 2018. Consensus Statement on the classification of tremors. from the task force on tremor of the International Parkinson and Movement Disorder Society. Mov. Disord. 33 (1), 75–87.

Coenen, V.A., Allert, N., Mädler, B., 2011. A role of diffusion tensor imaging fiber tracking in deep brain stimulation surgery: DBS of the dentato-rubro-thalamic tract (drt) for the treatment of therapy-refractory tremor. Acta Neurochir. (Wien) 153 (8), 1579–1585.

Coenen, V.A., Madler, B., Schiffbauer, H., et al., 2011. Individual fiber anatomy of the subthalamic region revealed with diffusion tensor imaging: a concept to identify the deep brain stimulation target for tremor suppression. Neurosurgery;68:1069-1075; discussion 1075-1066.

Coenen, V.A., Allert, N., Paus, S., et al., 2014. Modulation of the cerebello-thalamo-cortical network in thalamic deep brain stimulation for tremor: a diffusion tensor imaging study. Neurosurgery ;75:657-669; discussion 669-670.

Coenen, V.A., Rijntjes, M., Prokop, T., Piroth, T., Amtage, F., Urbach, H., Reinacher, P.C., 2016. One-pass deep brain stimulation of dentato-rubro-thalamic tract and subthalamic nucleus for tremor-dominant or equivalent type Parkinson's disease. Acta Neurochir (Wien) 158 (4), 773–781.

Coenen, V.A., Varkuti, B., Parpaley, Y., Skodda, S., Prokop, T., Urbach, H., Li, M., Reinacher, P.C., 2017. Postoperative neuroimaging analysis of DRT deep brain stimulation revision surgery for complicated essential tremor. Acta Neurochir (Wien) 159 (5), 779–787.

Coenen, V.A., Sajonz, B., Prokop, T., Reisert, M., Piroth, T., Urbach, H., Jenkner, C., Reinacher, P.C., 2020. The dentato-rubro-thalamic tract as the potential common deep brain stimulation target for tremor of various origin: an observational case series. Acta Neurochir (Wien) 162 (5), 1053–1066.

Dembek, T.A., Barbe, M.T., Åström, M., Hoevels, M., Visser-Vandewalle, V., Fink, G.R., Timmermann, L., 2017. Probabilistic mapping of deep brain stimulation effects in essential tremor. Neuroimage Clin 13, 164–173.

Edlow, B.L., Mareyam, A., Horn, A., Polimeni, J.R., Witzel, T., Tisdall, M.D., Augustinack, J.C., Stockmann, J.P., Diamond, B.R., Stevens, A., Tirrell, L.S., Folkerth, R.D., Wald, L.L., Fischl, B., van der Kouwe, A., 2019. 7 Tesla MRI of the ex vivo human brain at 100 micron resolution. Sci. Data 6 (1).

Eisinger, R.S., Wong, J., Almeida, L., Ramirez-Zamora, A., Cagle, J.N., Giugni, J.C., Ahmed, B., Bona, A.R., Monari, E., Wagle Shukla, A., Hess, C.W., Hilliard, J.D., Foote, K.D., Gunduz, A., Okun, M.S., Martinez-Ramirez, D., 2018. Ventral intermediate nucleus versus zona incerta region deep brain stimulation in essential tremor. Mov Disord Clin Pract 5 (1), 75–82.

Elias, G.J.B., Boutet, A., Joel, S.E., et al., 2021. Probabilistic mapping of deep brain stimulation: insights from 15 years of therapy. Ann. Neurol. 89, 426–443.

Ellerman, J.M., Flament, D., Kim, S.-G., Fu, Q.-G., Merkle, H., Ebner, T.J., Ugurbil, K., 1994. Spatial patterns of functional activation of the cerebellum investigated using high field (4 T) MRI. NMR Biomed. 7 (1-2), 63–68.

Ewert, S., Plettig, P., Li, N., Chakravarty, M.M., Collins, D.L., Herrington, T.M., Kühn, A. A., Horn, A., 2018. Toward defining deep brain stimulation targets in MNI space: a subcortical atlas based on multimodal MRI, histology and structural connectivity. NeuroImage 170, 271–282.

Fenoy, A.J., Schiess, M.C., 2017. Deep brain stimulation of the dentato-rubro-thalamic tract: outcomes of direct targeting for tremor. Neuromodul.: J. Int. Neuromodul, Soc. 20 (5), 429–436.

Fenoy, A.J., Schiess, M.C., 2018. Comparison of tractography-assisted to atlas-based targeting for deep brain stimulation in essential tremor. Mov. Disord. 33 (12), 1895–1901.

Flood, S., Jansen, J., 1966. The efferent fibres of the cerebellar nuclei and their distribution on the cerebellar peduncles in the cat. Acta Anat. (Basel) 63 (2), 137–166.

Fonov, V., Evans, A.C., Botteron, K., Almli, C.R., McKinstry, R.C., Collins, D.L., 2011. Unbiased average age-appropriate atlases for pediatric studies. NeuroImage 54 (1), 313–327.

Fytagoridis, A., Sandvik, U., Åström, M., Bergenheim, T., Blomstedt, P., 2012. Long term follow-up of deep brain stimulation of the caudal zona incerta for essential tremor. J. Neurol. Neurosurg. Psychiatry 83 (3), 258–262.

Gallay, M.N., Jeanmonod, D., Liu, J., Morel, A., 2008. Human pallidothalamic and cerebellothalamic tracts: anatomical basis for functional stereotactic neurosurgery. Brain Struct. Funct. 212 (6), 443–463.

Holslag, J.A.H., Neef, N., Beudel, M., Drost, G., Oterdoom, D.L.M., Kremer, N.I., van Laar, T., van Dijk, J.M.C., 2018. Deep brain stimulation for essential tremor: a comparison of targets. World Neurosurg. 110, e580–e584.

Horn, A., Reich, M., Vorwerk, J., Li, N., Wenzel, G., Fang, Q., Schmitz-Hübsch, T., Nickl, R., Kupsch, A., Volkmann, J., Kühn, A.A., Fox, M.D., 2017. Connectivity predicts deep brain stimulation outcome in Parkinson disease. Ann. Neurol. 82 (1), 67–78.

Horn, A., Li, N., Dembek, T.A., Kappel, A., Boulay, C., Ewert, S., Tietze, A., Husch, A., Perera, T., Neumann, W.-J., Reisert, M., Si, H., Oostenveld, R., Rorden, C., Yeh, F.-C., Fang, Q., Herrington, T.M., Vorwerk, J., Kühn, A.A., 2019. Lead-DBS v2: towards a comprehensive pipeline for deep brain stimulation imaging. NeuroImage 184, 293–316.

Husch, A., Petersen, M.V., Gemmar, P., Goncalves, J., Hertel, F., 2018. PaCER – a fully automated method for electrode trajectory and contact reconstruction in deep brain stimulation. Neuroimage Clin 17, 80–89.

Kim, W., Sharim, J., Tenn, S., et al., 2018. Diffusion tractography imaging-guided frameless linear accelerator stereotactic radiosurgical thalamotomy for tremor: case report. J. Neurosurg. 128, 215–221.

Kübler, D., Kroneberg, D., Al-Fatly, B., Schneider, G.-H., Ewert, S., van Riesen, C., Gruber, D., Ebersbach, G., Kühn, A.A., 2021. Determining an efficient deep brain stimulation target in essential tremor – cohort study and review of the literature. Parkinsonism Relat. Disord. 89, 54–62.

Küper, M., Thürling, M., Stefanescu, R., Maderwald, S., Roths, J., Elles, H.G., Ladd, M.E., Diedrichsen, J., Timmann, D., 2012. Evidence for a motor somatotopy in the cerebellar dentate nucleus–an FMRI study in humans. Hum. Brain Mapp. 33 (11), 2741–2749.

Louis, E.D., Ferreira, J.J., 2010. How common is the most common adult movement disorder? Update on the worldwide prevalence of essential tremor. Mov. Disord. 25 (5), 534–541.

Louis, E.D., Rios, E., Henchcliffe, C., 2010. How are we doing with the treatment of essential tremor (ET)?: Persistence of patients with ET on medication: data from 528 patients in three settings. Eur. J. Neurol. 17, 882–884.

Meola, A., Comert, A., Yeh, F.-C., Sivakanthan, S., Fernandez-Miranda, J.C., 2016. The nondecussating pathway of the dentatorubrothalamic tract in humans: human connectome-based tractographic study and microdissection validation. J. Neurosurg. 124 (5), 1406–1412.

Middlebrooks, E.H., Okromelidze, L., Carter, R.E., et al., 2021. Directed stimulation of the dentato-rubro-thalamic tract for deep brain stimulation in essential tremor: a blinded clinical trial. Neuroradiol. J., 19714009211036689.

Middlebrooks, E.H., Holanda, V.M., Tuna, I.S., Deshpande, H.D., Bredel, M., Almeida, L., Walker, H.C., Guthrie, B.L., Foote, K.D., Okun, M.S., 2018. A method for pre-operative single-subject thalamic segmentation based on probabilistic tractography for essential tremor deep brain stimulation. Neuroradiology 60 (3), 303–309.

Middlebrooks, E.H., Tuna, I.S., Almeida, L., Grewal, S.S., Wong, J., Heckman, M.G., Lesser, E.R., Bredel, M., Foote, K.D., Okun, M.S., Holanda, V.M., 2018. Structural connectivity-based segmentation of the thalamus and prediction of tremor

improvement following thalamic deep brain stimulation of the ventral intermediate nucleus. Neuroimage Clin. 20, 1266–1273.
Middlebrooks, E.H., Domingo, R.A., Vivas-Buitrago, T., Okromelidze, L., Tsuboi, T., Wong, J.K., Eisinger, R.S., Almeida, L., Burns, M.R., Horn, A., Uitti, R.J., Wharen, R. E., Holanda, V.M., Grewal, S.S., 2020. Neuroimaging advances in deep brain stimulation: review of indications, anatomy, and brain connectomics. AJNR Am. J. Neuroradiol. 41 (9), 1558–1568.
Middlebrooks, E.H., Lin, C., Okromelidze, L., Lu, C.-Q., Tatum, W.O., Wharen, R.E., Grewal, S.S., 2020. Functional activation patterns of deep brain stimulation of the anterior nucleus of the thalamus. World Neurosurg 136, 357–363.e2.
Middleton, F.A., Strick, P.L., 1998. Cerebellar output: motor and cognitive channels. Trends Cogn. Sci. 2 (9), 348–354.
Middleton, F.A., Strick, P.L., 2000. Basal ganglia and cerebellar loops: motor and cognitive circuits. Brain Res. Brain Res. Rev. 31, 236–250.
Morishita, T., Foote, K.D., Burdick, A.P., Katayama, Y., Yamamoto, T., Frucht, S.J., Okun, M.S., 2010. Identification and management of deep brain stimulation intra- and postoperative urgencies and emergencies. Parkinsonism Relat. Disord. 16 (3), 153–162.
Noecker, A.M., Frankemolle-Gilbert, A.M., Howell, B., et al., 2021. StimVision v2: examples and applications in subthalamic deep brain stimulation for Parkinson's disease. Neuromodul.: J. Int. Neuromodul. Soc. 24, 248–258.
Okun, M.S., Tagliati, M., Pourfar, M., Fernandez, H.H., Rodriguez, R.L., Alterman, R.L., Foote, K.D., 2005. Management of referred deep brain stimulation failures: a retrospective analysis from 2 movement disorders centers. Arch. Neurol. 62 (8), 1250–1255.
Papavassiliou, E., Rau, G., Heath, S., et al., 2004. Thalamic deep brain stimulation for essential tremor: relation of lead location to outcome. Neurosurgery 54:1120–1129; discussion 1129-1130.
Petersen, K.J., Reid, J.A., Chakravorti, S., Juttukonda, M.R., Franco, G., Trujillo, P., Stark, A.J., Dawant, B.M., Donahue, M.J., Claassen, D.O., 2018. Structural and functional connectivity of the nondecussating dentato-rubro-thalamic tract. NeuroImage 176, 364–371.
Pouratian, N., Zheng, Z., Bari, A.A., Behnke, E., Elias, W.J., DeSalles, A.A.F., 2011. Multi-institutional evaluation of deep brain stimulation targeting using probabilistic connectivity-based thalamic segmentation. J. Neurosurg. 115 (5), 995–1004.
Sammartino, F., Krishna, V., King, N.K.K., Lozano, A.M., Schwartz, M.L., Huang, Y., Hodaie, M., 2016. Tractography-based ventral intermediate nucleus targeting: novel methodology and intraoperative validation. Mov. Disord. 31 (8), 1217–1225.
Sandoe, C., Krishna, V., Basha, D., Sammartino, F., Tatsch, J., Picillo, M., di Biase, L., Poon, Y.-Y., Hamani, C., Reddy, D., Munhoz, R.P., Lozano, A.M., Hutchison, W.D., Fasano, A., 2018. Predictors of deep brain stimulation outcome in tremor patients. Brain Stimul. 11 (3), 592–599.
Sandvik, U., Koskinen, L.O., Lundquist, A., et al., 2020. Thalamic and subthalamic deep brain stimulation for essential tremor: where is the optimal target? Neurosurgery;70: 840-845; discussion 845-846.
Schönecker, T., Kupsch, A., Kühn, A.A., Schneider, G.-H., Hoffmann, K.-T., 2009. Automated optimization of subcortical cerebral MR imaging-atlas coregistration for improved postoperative electrode localization in deep brain stimulation. AJNR Am. J. Neuroradiol. 30 (10), 1914–1921.
Setsompop, K., Kimmlingen, R., Eberlein, E., Witzel, T., Cohen-Adad, J., McNab, J.A., Keil, B., Tisdall, M.D., Hoecht, P., Dietz, P., Cauley, S.F., Tountcheva, V., Matschl, V., Lenz, V.H., Heberlein, K., Potthast, A., Thein, H., Van Horn, J., Toga, A., Schmitt, F., Lehne, D., Rosen, B.R., Wedeen, V., Wald, L.L., 2013. Pushing the limits of in vivo diffusion MRI for the Human Connectome Project. NeuroImage 80, 220–233.
Tacyildiz, A.E., Bilgin, B., Gungor, A., Ucer, M., Karadag, A., Tanriover, N., 2021. Dentate nucleus: connectivity-based anatomic parcellation based on superior cerebellar peduncle projections. World Neurosurg. 152, e408–e428.
Thanvi, B., Lo, N., Robinson, T., 2006. Essential tremor-the most common movement disorder in older people. Age Ageing;35:344-349.
Tsuboi, T., Charbel, M., Peterside, D.T., Rana, M., Elkouzi, A., Deeb, W., Ramirez-Zamora, A., Lemos Melo Lobo Jofili Lopes, J., Almeida, L., Zeilman, P.R., Eisinger, R. S., Foote, K.D., Okromelidze, L., Grewal, S.S., Okun, M.S., Middlebrooks, E.H., 2021. Pallidal connectivity profiling of stimulation-induced dyskinesia in Parkinson's disease. Mov. Disord. 36 (2), 380–388.
Tsuboi, T., Wong, J.K., Eisinger, R.S., et al., 2021. Comparative connectivity correlates of dystonic and essential tremor deep brain stimulation. Brain 2021;144:1774–1786.
Vorwerk, J., Oostenveld, R., Piastra, M.C., Magyari, L., Wolters, C.H., 2018. The FieldTrip-SimBio pipeline for EEG forward solutions. Biomed. Eng. Online 17 (1). https://doi.org/10.1186/s12938-018-0463-y.
Wang, Q., Akram, H., Muthuraman, M., et al., 2021. Normative vs. patient-specific brain connectivity in deep brain stimulation. NeuroImage1;224:117307.
Wiesendanger, R., Wiesendanger, M., 1985. Cerebello-cortical linkage in the monkey as revealed by transcellular labeling with the lectin wheat germ agglutinin conjugated to the marker horseradish peroxidase. Exp. Brain Res. 59, 105–117.